Development 134, 1921-1930 (2007) doi:10.1242/dev.02851

Na,K-ATPase α2 and Ncx4a regulate zebrafish left-right patterning

Xiaodong Shu[1,*], Jie Huang[1,*], Yuan Dong[1,*], Jayoung Choi[1], Adam Langenbacher[1] and Jau-Nian Chen[1,2,3,4,†]

A conserved molecular cascade involving Nodal signaling that patterns the laterality of the lateral mesoderm in vertebrates has been extensively studied, but processes involved in the initial break of left-right (LR) symmetry are just beginning to be explored. Here we report that Na,K-ATPase α2 and Ncx4a function upstream of Nodal signaling to regulate LR patterning in zebrafish. Knocking down Na,K-ATPase α2 and Ncx4a activity in dorsal forerunner cells (DFCs), which are precursors of Kupffer's vesicle (KV), is sufficient to disrupt asymmetric gene expression in the lateral plate mesoderm and randomize the placement of internal organs, indicating that the activity of Na,K-ATPase α2 and Ncx4a in DFCs/KV is crucial for LR patterning. High-speed videomicroscopy and bead implantation experiments show that KV cilia are immobile and the directional fluid flow in KV is abolished in Na,K-ATPase α2 and Ncx4a morphants, suggesting their essential role in KV ciliary function. Furthermore, we found that intracellular Ca^{2+} levels are elevated in Na,K-ATPase α2 and Ncx4a morphants and that the defects in ciliary motility, KV fluid flow and placement of internal organs induced by their knockdown could be suppressed by inhibiting the activity of Ca^{2+}/calmodulin-dependent protein kinase II. Together, our data demonstrate that Na,K-ATPase α2 and Ncx4a regulate LR patterning by modulating intracellular calcium levels in KV and by influencing cilia function, revealing a previously unrecognized role for calcium signaling in LR patterning.

KEY WORDS: Left-right patterning, Calcium homeostasis, Cilia, Zebrafish

INTRODUCTION

The placement and anatomy of the internal organs are asymmetric with respect to the left-right (LR) axis in vertebrates, even though the external body plan appears to be bilaterally symmetrical. Evidence accumulated over the past decade has delineated a conserved cascade of molecular asymmetries, including *nodal*, *lefty1* (*lft1*), *lefty2* (*lft2*) and *pitx2*, in the lateral plate mesoderm (LPM). Disruption of the asymmetric expression pattern of these laterality genes causes abnormalities in the LR morphogenesis of the brain, heart and visceral organs in mouse, chick, frog and zebrafish (for reviews, see Burdine and Schier, 2000; Capdevila et al., 2000; Bisgrove and Yost, 2001).

Although the role of signals expressed asymmetrically in the LPM is relatively clear, the mechanisms that initially break LR symmetry are only beginning to be revealed. In *Xenopus*, the break in LR symmetry is evident as early as the first few cell divisions when 14-3-3 and H^+/K^+-ATPase proteins and serotonin become asymmetrically localized (Levin et al., 2002; Bunney et al., 2003; Fukumoto et al., 2005). However, similar asymmetric protein localization at this early developmental stage has not been noted in other vertebrate species, suggesting that mechanisms for the break of LR symmetry might have diverged among vertebrates (Levin et al., 2002; Kawakami et al., 2005; Adams et al., 2006).

In the chick, mouse and zebrafish models, the node has an essential role in LR patterning (Essner et al., 2002). In chick, a transient accumulation of extracellular Ca^{2+} on the left side of Henson's node induced by a gradient of H^+/K^+-ATPase-dependent membrane potential is required for the left-specific activation of Notch (Raya et al., 2004). In mammals, motile nodal cilia generate a leftward fluid flow (Nonaka et al., 1998; Okada et al., 2005). Disrupting the biogenesis or function of cilia in the node blocks nodal flow and induces LR patterning defects in the mouse (Nonaka et al., 1998; Marszalek et al., 1999; Okada et al., 1999; Takeda et al., 1999; McGrath et al., 2003; Okada et al., 2005). An asymmetric Ca^{2+} flux in tissues on the left edge of the node has been noted. The two-cilia model proposes that this asymmetric Ca^{2+} flux is a result of the activation of polycystin-2 (also known as polycystic kidney disease 2) cation channels by the leftward nodal flow (McGrath and Brueckner, 2003; McGrath et al., 2003; Tabin and Vogan, 2003), but the recent observation of leftward transportation of morphogens across the node offers an alternative view of how asymmetric Ca^{2+} flux might be initiated around the node (Tanaka et al., 2005; Raya and Belmonte, 2006; Shiratori and Hamada, 2006). In zebrafish, Kupffer's vesicle (KV), the equivalent of the node, also has a crucial role in LR patterning. Loss-of-function of intraflagellar transport proteins such as Ift88 (Polaris) and Ift57 (Hippi) inhibits the directional fluid flow in KV and induces randomization of organ placement in zebrafish (Amack and Yost, 2004; Bisgrove et al., 2005; Essner et al., 2005; Kramer-Zucker et al., 2005). As with the mouse model, an asymmetric Ca^{2+} flux is observed in cells surrounding the KV in zebrafish. Disrupting this asymmetric calcium signaling by treatment with thapsigargin, an inhibitor of sarco/endoplasmic reticulum ATPase (SERCA; also known as Atp2a1 – ZFIN), or by knocking down the activity of *ipk1* (*ippk* – ZFIN), causes abnormal LR patterning (Sarmah et al., 2005).

Ca^{2+} is an important signaling molecule for many biological processes. The levels of free Ca^{2+} in the cytoplasm are generally low in resting cells, but can be increased drastically upon stimulation (Berridge et al., 2000). Activation of plasma membrane calcium channels allows a small Ca^{2+} influx, which in turn leads to the activation of $InsP_3$ receptors or ryanodine receptors and the release

[1]Department of Molecular, Cell and Developmental Biology, [2]Molecular Biology Institute, [3]Jonsson Cancer Center and [4]Cardiovascular Research Laboratory, University of California, Los Angeles, CA 90095, USA.

*These authors contributed equally to this work
†Author for correspondence (e-mail: chenjn@mcdb.ucla.edu)

Accepted 14 March 2007

of a large quantity of Ca^{2+} from the endoplasmic reticulum (ER) or sarcoplasmic reticulum (SR). Once its signaling function has ended, Ca^{2+} is rapidly removed from the cytoplasm by SERCA, which returns Ca^{2+} to the ER/SR, and by the plasma membrane Ca^{2+}-ATPase (PMCA) and sodium-calcium exchanger (NCX), which extrude Ca^{2+} from the cell. Furthermore, as the Ca^{2+}-transporting activity of NCX is modulated by the levels of intracellular Na^+, Na,K-ATPase is also considered to be a calcium-regulating molecule. In fact, inhibition of Na,K-ATPase activity reduces the activity of NCX and results in an increase in the concentration of intracellular Ca^{2+} (for a review, see Blanco and Mercer, 1998), indicating that NCX and Na,K-ATPase cooperate to maintain a low intracellular Ca^{2+} level in resting cells.

We showed previously that morpholino (MO) knockdown of *Na,K-ATPase α2* (*atp1a2a* – ZFIN) induced cardiac laterality defects in zebrafish (Shu et al., 2003) and recent studies on the *heart and mind* (*Na,K-ATPase α1B1*; *atp1a1* – ZFIN) mutant also revealed an incompletely penetrant laterality phenotype in the visceral organs (Ellertsdottir et al., 2006), suggesting a role for the sodium pump in early LR patterning in zebrafish. Here, we investigate the mechanism by which the sodium pump regulates LR patterning in zebrafish. Our data show that Na,K-ATPase α2 and its functional partner Ncx4a, are involved in a very early step of LR patterning in zebrafish. Downregulation of Na,K-ATPase α2 and Ncx4a in dorsal forerunner cells (DFCs) and KV is sufficient to immobilize KV cilia, perturb directional fluid flow in KV, disrupt the asymmetric expression patterns of zebrafish laterality genes in the brain and LPM, and randomize the placement of all internal organs. We provide evidence that Na,K-ATPase α2 and Ncx4a are capable of modulating the intracellular calcium levels in zebrafish, consistent with the roles of these molecules defined previously by numerous biochemical and physiological studies in cultured cells and mammalian model organisms. We show that the phenotypes of those embryos with elevated intracellular Ca^{2+} levels induced by pharmacological means are identical to those observed in Na,K-ATPase α2 and Ncx4a morphants. Additionally, inhibiting calcium/calmodulin-dependent protein kinase II (CaMKII) activity was able to suppress the LR defects caused by A23187, thapsigargin, Na,K-ATPase α2-MO and Ncx4a-MO treatment, revealing a previously unacknowledged role for Na,K-ATPase α2/Ncx4a/CaMKII-mediated Ca^{2+} signaling in zebrafish LR patterning.

MATERIALS AND METHODS

Zebrafish

The TL strain was used for this study. Adult fish and embryos were maintained as previously described (Westerfield, 1995). Embryos for in situ hybridization were raised in the presence of 0.2 mM 1-phenyl-2-thiourea to maintain optical transparency (Westerfield, 1995).

Molecular cloning of Ncx4a

Total RNA was isolated from 80% epiboly embryos using the RNAqueous-4PCR Kit (Ambion, TX). The *ncx4a* fragment (equivalent to aa 443-609) was amplified by RT-PCR (95°C for 30 seconds, 60°C for 60 seconds, 72°C for 60 seconds, for 32 cycles) with the following primers: 5′-ACTATCGCACAGAGGATGGCA-3′ and 5′-GTCTCATCATTGAGGAACTCC-3′.

The 3′ sequence of *ncx4a* (equivalent to aa 84-938) was amplified by RT-PCR (95°C for 30 seconds, 58°C for 60 seconds, 72°C for 120 seconds, for 35 cycles) with primers: 5′-CTCATCTACATGTTTCTGGGC-3′ and 5′-CTGTCTGCGTAAGAAGCGACATGT-3′. The 5′ sequence of *ncx4a* (equivalent to aa 1-473) was derived from 5′-RACE using the SMART RACE cDNA Amplification Kit (BD Biosciences, CA) with the primer 5′-TGAGCTCCTTAACCGTCTCTCCTG-3′. All PCR products were cloned into the pCRII-TOPO vector (Invitrogen, CA) and confirmed by sequencing. pCRII-TOPO-Ncx4a/443-609 was linearized with *Bam*HI and T7 RNA polymerase was used to make the antisense probe for *ncx4a*.

Morpholinos

Morpholino antisense oligonucleotides (MOs) complementary to the translation start site and its flanking sequence of mRNAs encoding Na,K-ATPase α2 (α2-MO, 5′-TTTCATGTCCGTACCCTTTCCCCAT-3′) and Ncx4a (Ncx4a-MO, 5′-AAAGGCGCAGATGAAACATGGTGGC-3′) or to the splice-acceptor sites of Na,K-ATPase α2 (α2-SP-MO, 5′-CAACCTATGAAAGACAGACAAGTGG-3′) and Ncx4a (Ncx4a-SP-MO, 5′-CAACCTGCATACAGGAGCAGTGTTT-3′) were synthesized by GeneTools. An MO with a 5 bp mismatch to α2-MO (CTL-MO, 5′-TTTgATcTCCGTAgCCTTTgCCgAT-3′) was used as a control (lowercase letters indicate mismatched bases). Wild-type embryos were injected with 2 ng α2-MO, 4.5 ng α2-SP-MO, 4 ng Ncx4a-MO or 5 ng Ncx4a-SP-MO at the 1-cell stage. The injected embryos were fixed at the 15- to 16-somite stage (for *spaw*), 21- to 22-somite stage (for *lft1/2*), 23- to 24-somite stage (for *pitx2*), or after 2 days of development (for *cmlc2* and *fkd2*) for whole-mount in situ hybridization to analyze gene expression patterns and internal organ laterality.

To knockdown the activities of Na,K-ATPase α2 and Ncx4a specifically in DFCs, α2-MO or Ncx4a-MO tagged with fluorescein was injected into the yolk of 128-cell stage embryos. After 2 days of development, the laterality of heart and visceral organs was examined by whole-mount in situ hybridization using *cmlc2* and *fkd2* probes in those injected embryos having fluorescent signals in DFCs/KV.

Primer pairs used in RT-PCR to investigate the knockdown efficiency of α2-SP-MO and Ncx4a-SP-MO are: 5′-CTTCAGATAAATGCAGAGGAGG-3′ and 5′-ACCCAAAGTCTCCACAGCTTC-3′; 5′-TAGGAAGGTGGTGAGCTGCC-3′ and 5′-CCAGTTTGGTGTGCTCTCCC-3′; these pairs yield 875 bp (normal splicing) or 360 bp (skip exon 2), and 573 bp (normal splicing) or 455 bp (skip exon 7), respectively.

Constitutive activation of CaMKII

The coding region for CaMKIIδCT287D (kindly provided by J. Brown, University of California, San Diego, La Jolla, CA) was subcloned into the *Eco*RI site of the pcGlobin2 vector (Ro et al., 2004) to create pcGlobin2-CaMKIIδCT287D, which was then linearized with *Apa*I. mRNA of CaMKIIδCT287D was transcribed using mMESSAGE mMACHINE (Ambion) and injected into zebrafish embryos at the 1-cell stage.

In situ hybridization

Whole-mount in situ hybridization was performed as described (Chen and Fishman, 1996). The laterality of the heart and visceral organs was determined by double in situ hybridization with *cmlc2* and *fkd2*. The other antisense RNA probes used in this study were *spaw* (from M. Rebagliati, University of Iowa, Iowa City, IA), *lrdr*, *lft1*, *lft2*, *pitx2* (from H. J. Yost, University of Utah, Salt Lake City, UT), *ntl*, *Na,K-ATPase α2* and *ncx4a*.

Immunostaining

KV cilia were visualized by immunostaining using anti-acetylated tubulin (Sigma, MO) as previously described (Essner et al., 2002). Images were acquired with an LSM510 confocal microscope (Zeiss, Germany).

Chemical treatment

Chemicals used in this study are thapsigargin (0.5 μM, Sigma), A23187 (13 nM, Sigma) and KN62 (20 μM, Calbiochem, CA). Unless otherwise indicated, chemicals were added to the embryo media (5 mM NaCl, 0.17 mM KCl, 0.33 mM $CaCl_2$, 0.33 mM $MgSO_4$) at 3 hours post-fertilization (hpf) and washed away at 6 hpf by extensive rinsing with embryo medium. Embryos were then fixed at day 2 and the laterality of the heart and visceral organs examined as described above.

Fluorescent bead injections

Fluorescent beads of 0.2 μm diameter (Fluorspheres 580/605, Molecular Probes) were diluted 1:100 in 1×PBS. About 0.3 nl of beads were injected into KV at the 7- to 10-somite stage. Embryos were imaged on a Zeiss Axioplan 2 microscope equipped with a 40× water immersion lens.

Calcium imaging

Embryos used for calcium imaging were injected with 1 nl of a mixture of 50 mM Calcium Green dextran (as a calcium indicator) and 0.05% (w/v) tetramethylrhodamine dextran (as an internal control for injection) (Molecular Probes). 2 ng of α2-MO or 4 ng of Ncx4a-MO were co-injected with the mixture of Calcium Green and rhodamine dextran to create Na,K-ATPase α2 and Ncx4a morphants. Images of Calcium Green and rhodamine in blastomeres of control embryos and Na,K-ATPase α2 and Ncx4a morphants were acquired with an LSM510 confocal microscope (Zeiss, Germany) at the blastula stage. Fluorescence intensities of Calcium Green and rhodamine in each embryo were analyzed with MetaMorph (Molecular Device Corporation). To normalize for variations between injections, the calcium intensity among embryos was compared based on the ratio of the intensity of the Calcium Green and rhodamine signals.

High-speed videomicroscopy

Footage was captured using a 63× water immersion lens on a Zeiss AxioplanII microscope (Zeiss, Germany) equipped with a high-speed video camera (RedLake Motion Meter, RedLake MASD, San Diego). Movies of KV cilia were acquired at 250 frames per second and played back at 30 frames per second.

RESULTS

Na,K-ATPase α2 is required for LR patterning in zebrafish

We showed previously that the activity of Na,K-ATPase α2 is required for establishing proper cardiac laterality in zebrafish (Shu et al., 2003). To evaluate whether Na,K-ATPase α2 regulates the laterality of visceral organs, we injected an MO targeting the translation initiation site of Na,K-ATPase α2 (α2-MO) into wild-type zebrafish embryos at the 1-cell stage and analyzed the positions of the internal organs by in situ hybridization using *cmlc2* (*myl7* – ZFIN) to visualize the heart and *fkd2* (*foxa3* - ZFIN) for the gut, liver and pancreas. After 2 days of development, the cardiac ventricle is placed to the right of the atrium (cardiac looping), and a leftward bend of the developing intestine (gut looping) positions the gut and liver on the left side of the embryo and the pancreas on the right. As we reported previously, Na,K-ATPase α2 morphants (referred to as α2 morphants) do not have apparent morphological defects besides abnormalities in cardiac looping (Fig. 1B) (Shu et al., 2003). Specifically, 21% of α2 morphants had reversed cardiac looping and the hearts of 26% never underwent looping (n=122) (Fig. 1E-G,K). In addition to the cardiac looping abnormality, knocking down the activity of Na,K-ATPase α2 induced laterality defects in visceral organs. 27% of α2 morphants had reversed positioning of the gut, liver and pancreas and 11% of the α2-MO-injected embryos did not undergo gut looping (n=122) (Fig. 1H-K). Furthermore, the laterality defects of the heart and visceral organs were not concordant with each other. In 45% of α2 morphants, organ positions were normal (situs solitus), 13% were completely reversed (situs inversus) and 42% had discordant positions of the heart and visceral organs (heterotaxia). Similar laterality defects were also observed in embryos injected with α2-SP-MO, an MO targeting the splice-acceptor site of exon 7 (43% abnormal cardiac and 42% abnormal gut looping, n=96) (Fig. 1K), but such laterality defects were not observed in embryos injected with a control α2 MO containing 5 mismatches (CTL-MO). Only 6% of CTL-MO-injected embryos exhibited cardiac laterality defects and 5% had reversed visceral organs (n=103). These results demonstrate that Na,K-ATPase α2 is required for the establishment of proper laterality of both the visceral organs and the heart in zebrafish.

To investigate whether the activity of Na,K-ATPase α2 is required for establishing asymmetric gene expression in the LPM, we analyzed expression of laterality genes in α2 morphants.

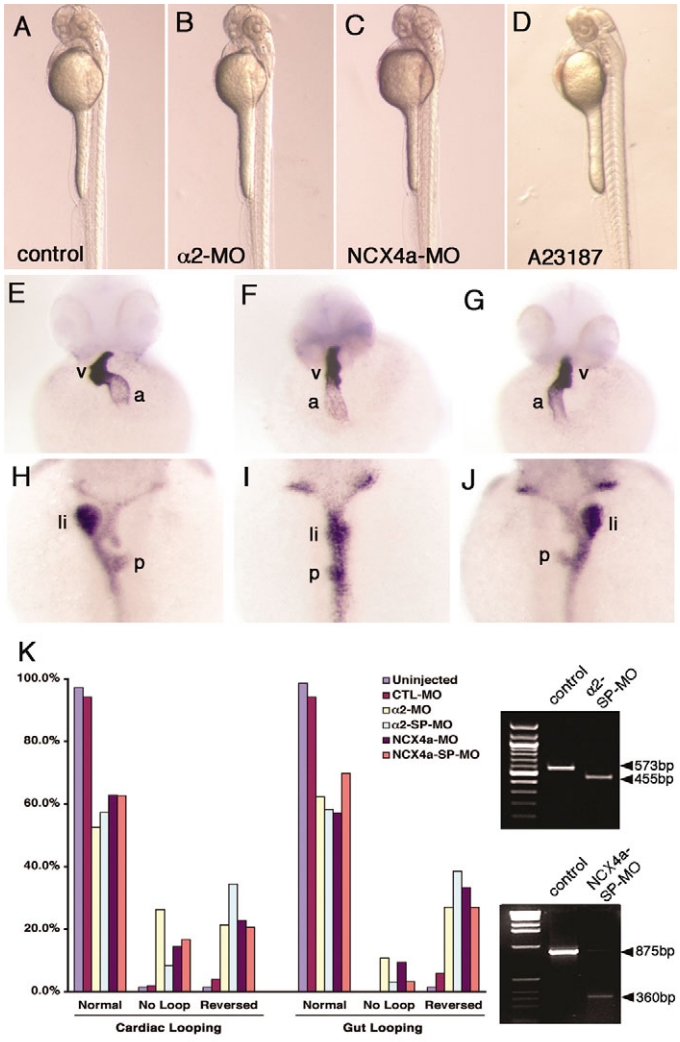

Fig. 1. Na,K-ATPase α2 is required for heart and gut LR patterning in zebrafish. (**A-D**) Live 2-day-old control (A), α2 morphant (B), Ncx4a morphant (C) and A23187-treated (D) embryos. (**E-G**) α2 morphants that exhibited normal (E), absent (F) or reversed (G) cardiac looping after 2 days of development. Ventral view, with anterior to the top. v, ventricle; a, atrium. (**H-J**) 2-day-old α2 morphants with normal (H), straight (I) or reversed (J) positions of gut, liver and pancreas. Dorsal view, with anterior to the top. li, liver; p, pancreas. (**K**) Bar chart detailing the heart and gut laterality phenotypes of uninjected embryos and those injected with CTL-MO, α2-MO, α2-SP-MO, Ncx4a-MO and Ncx4a-SP-MO. The effects of α2-SP-MO and Ncx4a-SP-MO on RNA processing are shown in the upper and lower panels, respectively, on the right.

Whereas some embryos had normal left-sided expression of *spaw* and *pitx2*, transcripts of these genes were detected on the right-hand side, bilaterally, or not at all in the LPM of other α2 morphants (Fig. 2A-H; Table 1). The expression of *lft1* and *lft2* in the left LPM was also disrupted in α2 morphants; but surprisingly, rather than showing a randomized expression pattern, the expression of *lft1/2* was absent in most of the α2 morphants. Occasionally, we detected *lft1/2* expression in either the left (normal) or right (reversed) LPM of α2 morphants, but never bilaterally (Fig. 2I-N; Table 1). In addition to the left LPM, *lft1* was also expressed in the left habenula in the developing zebrafish brain. We found that *lft1* expression in

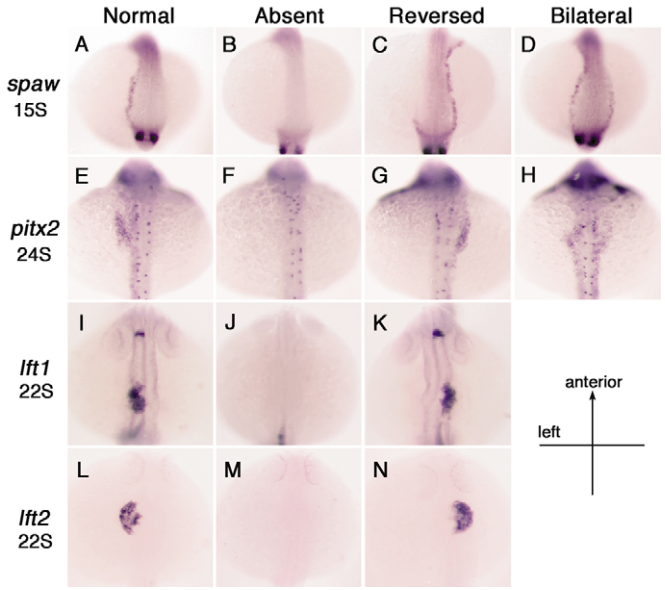

Fig. 2. Na,K-ATPase α2 is required for asymmetric gene expression in zebrafish. Examples of *spaw* (**A-D**), *pitx2c* (**E-H**), *lft1* (**I-K**) and *lft2* (**L-N**) expression pattern in α2-MO-injected embryos at the 15-, 22- or 24-somite stage. Dorsal view, anterior to the top.

the brain was also absent in a large fraction of α2 morphants (49%, *n*=75) (Fig. 2I-K). These data demonstrate that downregulating the activity of Na,K-ATPase α2 disrupts the asymmetric expression patterns of zebrafish laterality genes and randomizes the placement of multiple internal organs, indicating that the activity of Na,K-ATPase α2 is required for an early step of LR patterning in zebrafish.

The asymmetric expression patterns of *spaw*, *pitx2* and *lft1/2* are usually regulated concordantly (Schier, 2003). However, in α2 morphants, there was an unusual discordant expression of *spaw* and *pitx2* (randomization) and of *lft1/2* (absent). We investigated whether this was due to a global repression of *lft1/2* expression in α2 morphants. As shown in Fig. 3, the expression of *lft1/2* during gastrulation, as well as the midline expression of *lft1* in the segmentation period, were not affected in α2 morphants. These findings indicate that the absence of *lft1/2* expression in the LPM and habenula is a result of LR patterning defects, rather than a general suppression of their expression induced by the downregulation of Na,K-ATPase α2.

The fish-specific sodium calcium exchanger Ncx4a is required for LR patterning

Calcium signaling has been implicated as an early determinant of LR patterning (Fujinaga et al., 1994; Toyoizumi et al., 1997; McGrath et al., 2003; Raya et al., 2004). One well-characterized function of Na,K-ATPase is to regulate the intracellular Ca^{2+} level by modulating the activity of NCX (Blanco and Mercer, 1998; Blaustein and Lederer, 1999). Therefore, we investigated whether Na,K-ATPase α2 regulates LR patterning by functionally coupling with NCX. We identified six zebrafish homologs of NCX from the zebrafish Ensemble database. Phylogeny analysis indicates that these homologs represent two Ncx1s (Ncx1h and Ncx1n; ZFIN annotation Slc8a1a and Slc8a1b, respectively) (Langenbacher et al., 2005), one Ncx2 (ZFIN annotation Slc8a2), one Ncx3 (ZFIN annotation Slc8a3) and two Ncx4s (Ncx4a and Ncx4b; ZFIN annotation Slc8a4a and Slc8a4b, respectively) (Fig. 4A). Interestingly, whereas homologs of Ncx1, 2 and 3 exist in other vertebrate species, the Ncx4s appear to be fish-specific (Marshall et al., 2005).

Table 1. α2-MO and NCX4a-MO injections disrupt asymmetric gene expression in the LPM

Treatment	# of embryos	Left (%)	Right (%)	Absent (%)	Bilateral (%)
spaw					
Uninjected	92	98	0	2	0
CTL-MO	64	98	0	2	0
α2-MO	118	28	23	20	29
α2-MO (DFC)	106	30	18	16	36
NCX4a-MO	126	29	24	25	22
NCX4a-MO (DFC)	110	30	21	18	31
α2-MO+NCX4a-MO	109	33	20	17	30
A23187	114	33	19	27	21
pitx2					
Uninjected	81	98	1	1	0
CTL-MO	77	99	1	0	0
α2-MO	94	39	28	20	13
α2-MO (DFC)	92	38	25	17	20
NCX4a-MO	100	37	24	31	8
NCX4a-MO (DFC)	94	42	22	19	17
α2-MO+NCX4a-MO	88	34	24	22	20
A23187	102	36	22	20	22
lft1					
Uninjected	87	75	3	22	0
CTL-MO	75	72	1	27	0
α2-MO	115	22	8	70	0
α2-MO (DFC)	94	24	10	66	0
NCX4a-MO	95	24	15	61	0
NCX4a-MO (DFC)	90	24	15	61	0
α2-MO+NCX4a-MO	98	25	8	66	1
A23187	98	5	4	91	0
lft2					
Uninjected	99	80	3	17	0
CTL-MO	85	80	0	20	0
α2-MO	89	13	7	80	0
α2-MO (DFC)	93	13	11	74	2
NCX4a-MO	109	30	10	60	0
NCX4a-MO (DFC)	88	28	11	60	1
α2-MO+NCX4a-MO	90	20	11	68	1
A23187	104	16	3	78	3

Laterality gene expression in wild-type, CTL-MO, α2-MO or NCX4a-MO embryos. The expression patterns of *spaw*, *pitx2* and *lft1/2* in the lateral plate mesoderm were analyzed at the 15-, 24- and 22-somite stages, respectively. The expression patterns are scored either as left-sided (normal), right-sided (reversed), absent or bilateral. Data presented are collected from at least four independent experiments.

Our data showed that Na,K-ATPase α2 activity is required for proper asymmetric expression of *spaw*, which is already evident by the 12-somite stage in zebrafish (Long et al., 2003). Therefore, NCXs that act as functional partners of Na,K-ATPase α2 in LR decisions should be expressed early during embryogenesis. In situ hybridization analysis showed that *ncx1h* is a cardiac-specific gene whose expression is first detected in the bilateral cardiac primordia at the 12-somite stage (Langenbacher et al., 2005), *ncx2* is not expressed during embryogenesis (not shown), and *ncx4b* expression is restricted to the hypaxial muscle and to some head mesenchymes after 2 days of development (Fig. 4C). Therefore, these genes are not likely to cooperate with Na,K-ATPase α2 in LR patterning. However, *ncx1n*, *ncx3* and *ncx4a* are expressed ubiquitously during gastrulation and early somitogenesis stages, and thus are potential

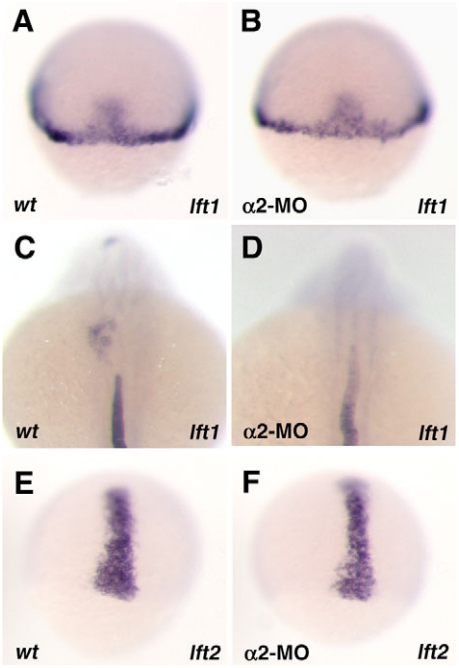

Fig. 3. The expression of *lft1* and *lft2* in zebrafish α2 morphants. Examples of *lft1* (**A-D**) and *lft2* (**E**,**F**) expression in wild type (wt, A,C,E) and α2 morphants (B,D,F) at the shield stage (A,B), 75% epiboly (E,F) and 22-somite stage (C,D).

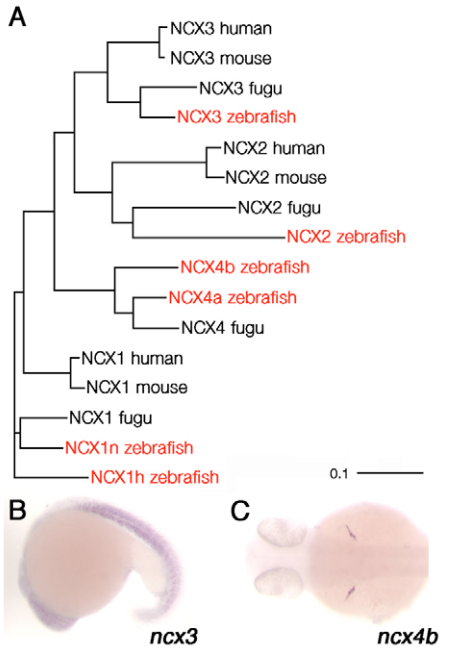

Fig. 4. Phylogenetic analysis of zebrafish NCX isoforms and expression patterns of *ncx3* and *ncx4b*. (**A**) The sequences of zebrafish *ncx1h*, *ncx1n*, *ncx3* and *ncx4a* were derived from RACE and RT-PCR. Full-length zebrafish *ncx2* and *ncx4b* sequences were obtained from the Ensembl Genome Browser. The amino acid sequences of human, mouse and fugu NCX isoforms are the same as those used by Marshall et al. (Marshall et al., 2005). Sequence alignments and phylogenetic analyses were performed using ClustalX. The unit of the scale bar represents 10% amino acid substitution per site. (**B**) *ncx3* is expressed predominantly in the somites in 1-day-old zebrafish embryos. (**C**) *ncx4b* expression is restricted in the hypaxial muscle after 3 days of development.

functional partners of Na,K-ATPase α2 in LR patterning. After 1 day of development, *ncx4a* expression remains ubiquitous (Fig. 5), whereas *ncx1n* and *ncx3* transcripts are predominantly detected in the neural tissues (Langenbacher et al., 2005) and somites (Fig. 4B), respectively.

We knocked down the activities of Ncx1n, Ncx3 and Ncx4a by injecting MOs targeting the translation initiation sites of their mRNAs into wild-type zebrafish embryos at the 1-cell stage. Whereas MOs targeting *ncx1n* or *ncx3* did not induce any noticeable morphological abnormalities, embryos injected with the Ncx4a-MO exhibited phenotypes similar to the α2 morphants. The general morphology of Ncx4a morphants was normal (Fig. 1C), but the expression domains of *spaw* and *pitx2* were randomized (Table 1). In addition, whereas the midline expression of *lft1/2* was unaffected (data not shown), their expression in the lateral mesoderm and habenula was absent in the majority of Ncx4a-MO-injected embryos (Table 1). Furthermore, the position of the heart and visceral organs was disrupted. 46% of the embryos injected with Ncx4a-MO had laterality defects (n=180). Specifically, 23% of Ncx4a morphants had reversed cardiac looping and 14% had a straight heart tube at the midline. 33% of the Ncx4a-MO-injected embryos had reversed positioning of the visceral organs and the gut failed to loop in 9% of these embryos (Fig. 1K). As we observed in α2 morphants, the looping of the heart and gut of Ncx4a morphants were not concordant with each other. 26% of the Ncx4a-MO-injected embryos had heterotaxia and 21% had situs inversus. Similar laterality defects in asymmetric gene expression and the placement of internal organs were observed in embryos injected with Ncx4a-SP-MO, an MO targeting the splice-acceptor site of exon 2 of *ncx4a* (37% abnormal cardiac, 30% abnormal gut looping, n=126) (Fig. 1K). These data demonstrate that as with Na,K-ATPase α2, the activity of Ncx4a is required for proper LR patterning in zebrafish.

Cooperative effect of Ncx4a and Na,K-ATPase α2 in LR patterning

The similarity of the Na,K-ATPase α2- and Ncx4a-knockdown phenotypes and their shared physiological role in modulating intracellular Ca^{2+} levels suggest that Na,K-ATPase α2 might function cooperatively with Ncx4a to regulate LR patterning. We co-injected α2- and Ncx4a-MOs into zebrafish embryos and analyzed their effects on LR patterning. Whereas injecting 0.5 ng of α2-MO or 2 ng of Ncx4a-MO into wild-type embryos did not cause significant laterality defects, co-injection of these amounts of α2-MO and Ncx4a-MO effectively induced randomized placement of the internal organs (44% heterotaxia, n=140) (Fig. 5G). In addition, *spaw* and *pitx2* expression patterns were randomized and *lft1/2* expression was absent in α2 and Ncx4a double morphants (Table 1). This further supports the notion that Na,K-ATPase α2 and Ncx4a function cooperatively to regulate LR patterning in zebrafish.

Na,K-ATPase α2 and Ncx4a in DFCs are required for directional fluid flow in KV

In situ hybridization analysis revealed that the genes encoding Na,K-ATPase α2 and Ncx4a are expressed in a broad range of tissues during the gastrula period and early somitogenesis, including KV (Fig. 5B,E), which is the equivalent of the mammalian node in teleosts (Essner et al., 2002; Essner et al., 2005; Kramer-Zucker et al., 2005). To investigate whether Na,K-ATPase α2 and Ncx4a regulate zebrafish LR patterning by modulating the formation and/or

function of KV, we injected fluorescein-conjugated α2-MO or Ncx4a-MO into the yolk at the early blastula stage (128-cell stage) to target the precursors of KV, the DFCs (Amack and Yost, 2004). Embryos injected with MO at the 128-cell stage accumulated strong fluorescent signals in DFCs (Fig. 6B), and developed cardiac looping defects (α2-MO: 15% straight and 27% reversed, n=135; Ncx4a-MO: 13% straight and 28% reversed, n=112) (Fig. 6A) in association with the absence of *lft1/2* and randomized *spaw* and *pitx2* expression (Table 1). By contrast, 91% of CTL-MO-injected embryos were normal (n=111) (Fig. 6A). MO injected into the yolk at the 128-cell stage can be incorporated into DFCs as well as localized to yolk nuclei (Cooper and D'Amico, 1996). To investigate whether the LR defects observed were due to the knockdown of Na,K-ATPase α2 and Ncx4a activity in DFCs, we injected fluorescein-conjugated α2-MO or Ncx4a-MO into the yolk at the dome stage; at this time, the DFCs are no longer connected directly to the yolk (Cooper and D'Amico, 1996). We did not detect fluorescent signals in DFCs of these embryos (Fig. 6C) and did not observe a randomization of the placement their internal organs (88% of α2-MO and 91% of Ncx4a-MO-injected embryos had normal situs; n=133 and 143, respectively), indicating that the activities of Na,K-ATPase α2 and Ncx4a are crucial in DFCs for LR patterning in zebrafish.

The formation and migration of DFCs appeared to be normal as indicated by *ntl* expression (Fig. 6D,E), and the KV does form in α2 (Fig. 6G) and Ncx4a morphants (not shown). The expression of KV markers such as *lrdr* (*dnah9* – ZFIN) is also normal in α2 and Ncx4a morphants (not shown). Furthermore, after analyzing 798 KV cilia in 12 embryos, we did not detect significant differences in the number or length of KV cilia between control embryos and α2 morphants (4.12±0.22 μm in length and 71±18 cilia per KV in controls versus 3.93±0.66 μm in length and 62±19 cilia per KV in α2 morphants, P>0.1) (Fig. 6H,I). Together, these data indicate that Na,K-ATPase α2 and Ncx4a do not control laterality through a role in the formation of KV or KV cilia. We then investigated whether Na,K-ATPase α2 and Ncx4a are required for proper function of KV, and found that the motility of KV cilia was severely defective in α2 and Ncx4a morphants. Of the 35 uninjected control embryos analyzed, 33 had many motile cilia in KV (see Movie 1 in the supplementary material). However, we did not observe any motile KV cilia in 27 of the 31 α2 morphants inspected (see Movie 2 in the supplementary material). Furthermore, whereas strong counterclockwise fluid flow was detected inside KV in all CTL-MO-injected embryos that were successfully implanted with fluorescent beads (Table 2; Movie 3 in the supplementary material), directional fluid flow was not observed in α2 (Table 2; Movie 4 in the supplementary material) and Ncx4a (not shown) morphants.

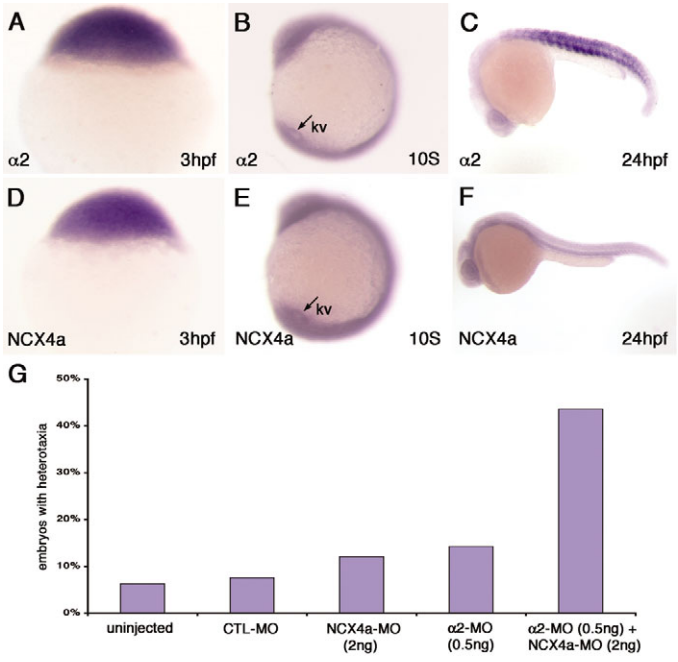

Fig. 5. Ncx4a is required for heart and gut LR patterning in zebrafish. (**A-F**) Expression pattern of the genes encoding Na,K-ATPase α2 and Ncx4a. Transcripts encoding Na,K-ATPase α2 (A) and Ncx4a (D) are detected prior to the mid-blastula stage. By the 10-somite stage, Na,K-ATPase α2 (B) and Ncx4a (E) are expressed in a broad range of tissues including Kupffer's vesicle (kv, arrow). By the 24-somite stage, Na,K-ATPase α2 is expressed predominantly in the somites (C), whereas Ncx4a remains ubiquitous (F). (**G**) Bar chart of the percentage of embryos exhibiting heart and/or gut laterality defects.

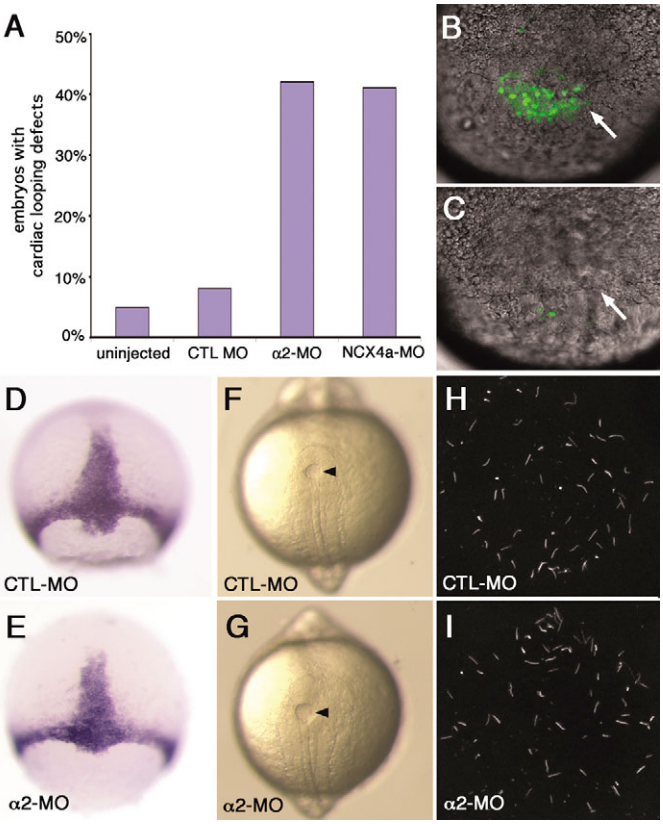

Fig. 6. Na,K-ATPase α2 and Ncx4a in DFCs/KV are required for LR patterning. (**A**) Morpholino knockdown of genes encoding Na,K-ATPase α2 or Ncx4a in DFCs induces LR patterning defects in zebrafish. Bar chart shows the percentage of embryos injected with α2-MO or Ncx4a-MO developing cardiac looping defects. (**B**,**C**) Fluorescent signals of the α2-MO accumulated in DFCs in embryos injected with the MO at the 128-cell stage (B), but were largely excluded from DFCs when the injection was done at the dome stage (C). Arrows point to DFCs. (**D**,**E**) The expression pattern of *ntl* in α2 morphants (E) is similar to that observed in CTL-MO-injected embryos (D). (**F**,**G**) The morphology of KV (arrowheads) appears normal in control (F) and α2-MO-injected (G) embryos. (**H**,**I**) Anti-acetylated tubulin staining shows that cilia are present in KV of control (H) and α2-MO-injected (I) embryos.

Table 2. α2-MO and NCX4a-MO injections disrupt fluid flow in KV

Treatment	# of successful bead injections	# of embryos with strong KV flow	# of embryos without KV flow
CTL-MO	16	16 (100%)	0 (0%)
α2-MO	42	1 (2%)	41 (98%)
NCX4a-MO	19	2 (11%)	17 (89%)
α2-MO+KN62	24	17 (71%)	7 (29%)

Taken together, these data provide evidence that the activities of Na,K-ATPase α2 and Ncx4a are required for KV ciliary motility and confirm the correlation between directional fluid flow and LR patterning.

CaMKII mediates calcium-induced LR defects

NCX is the primary molecule used by cells to extrude calcium, and Na,K-ATPase modulates the activity of NCX (Blaustein and Lederer, 1999). Knocking down the activity of Ncx4a or Na,K-ATPase α2 is thus predicted to slightly increase the level of intracellular calcium. This notion is supported by the finding that Ca^{2+} levels in the blastomeres of α2 and Ncx4a morphants are 1.24-fold and 1.14-fold higher than in control embryos ($P<0.01$, $n=12$ and $P<0.05$, $n=16$, respectively) (Fig. 7A). In addition, the phenotypes of Ncx4a or α2 morphants are similar to those of embryos treated with A23187, a calcium ionophore that allows calcium influx from extracellular sources. Incubating embryos with low levels of A23187 (13 nM) disrupted the asymmetric expression patterns of *spaw*, *pitx2* and *lft1/2* (Table 1) and induced cardiac looping defects (16% straight and 29% reversed, $n=112$), but did not affect general morphogenesis of zebrafish embryos (Fig. 1D), a phenotype similar to that of α2 and Ncx4a morphants. This effect is calcium-dependent, as the incidence of embryos with LR defects was significantly reduced when treatment with A23187 was performed in embryo media from which calcium chloride had been omitted (13% abnormal, $n=130$) (Fig. 7B). In addition to A23187, thapsigargin, a SERCA-inhibitor that blocks the resequestration of Ca^{2+} into the sarco/endoplasmic reticulum, is often used to manipulate intracellular Ca^{2+} levels. We found that treating embryos with a low dose of thapsigargin (0.5 μM) could also induce cardiac looping defects (8% straight and 41% reversed, $n=112$) without affecting other aspects of morphogenesis (Fig. 7B), further supporting the notion that the intracellular Ca^{2+} level plays a crucial role in LR patterning.

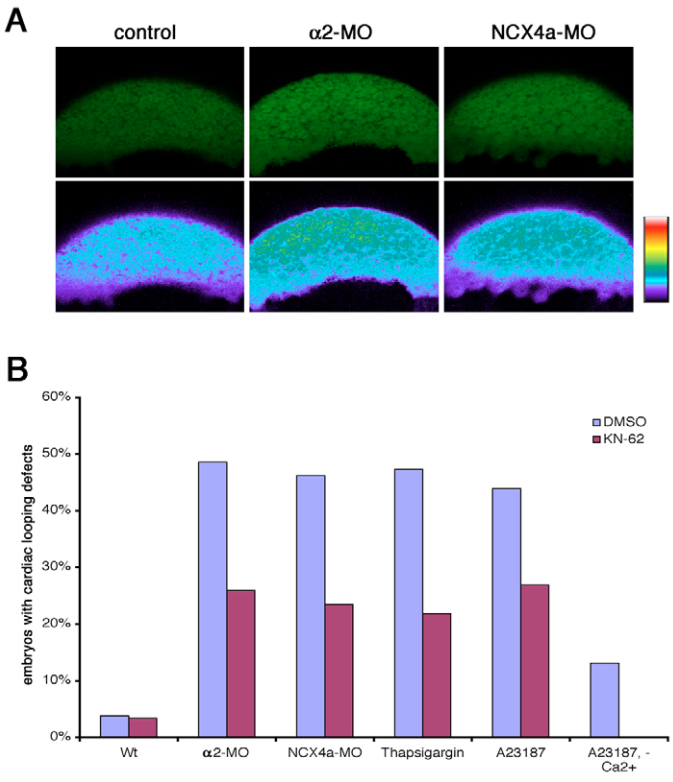

Fig. 7. CaMKII inhibition suppresses LR defects induced by altered Ca^{2+} levels. (**A**) Confocal imaging of Calcium Green in blastomeres of control zebrafish embryos (left) and those injected with α2-MO (middle) and Ncx4a-MO (right). The upper panels show the original fluorescent images and the lower panels are false-colored to highlight the increased Ca^{2+} levels in α2 and Ncx4a morphants. (**B**) CaMKII mediates Ca^{2+} signaling in LR patterning. Bar chart shows the percentage of embryos exhibiting LR patterning defects. Treatment with the CaMKII-inhibitor KN62 is able to block LR patterning defects induced by α2-MO, Ncx4a-MO, A23187 or thapsigargin.

Calcium/calmodulin-dependent protein kinase II (CaMKII) is an essential downstream mediator of calcium signaling (Berridge et al., 2000). To investigate whether CaMKII mediates Na,K-ATPase α2 and Ncx4a-dependent signaling in LR patterning, we tested whether increased CaMKII activity could induce LR defects. We injected mRNA encoding CaMKIIδCT287D, a mutant form of CaMKII that has constitutive Ca^{2+}-independent activity (Brickey et al., 1994; Pfleiderer et al., 2004), into zebrafish embryos at the 1-cell stage and observed dosage-dependent LR defects. Normally, the primitive heart tube protrudes to the left of the embryo (cardiac jogging) at 24 hpf in zebrafish (Chen et al., 1997). We found that whereas 35% and 48% of embryos receiving 10 pg and 20 pg of CaMKIIδCT287D mRNA exhibited abnormal jogging, respectively (10 pg injection: 13% no jog and 22% right-jog, $n=78$; 20 pg injection: 26% no jog and 22% right-jog, $n=94$), 69% of embryos receiving 50 pg of mRNA had abnormal jogging (51% no jog and 18% right-jog, $n=49$), indicating that the activation of CaMKII can indeed induce laterality defects.

We further investigated whether inhibiting CaMKII could suppress the LR defects induced by thapsigargin, A23187, α2-MO or Ncx4a-MO knockdown. KN62 is a well-characterized CaMKII inhibitor. We found that treatment with 20 μM KN62 did not cause noticeable morphological defects in wild-type embryos but could significantly reduce the incidence of the cardiac looping defects induced by α2-MO, Ncx4a-MO, thapsigargin or A23187. Only 22% of the embryos co-treated with thapsigargin and KN62 (6% straight and 16% reversed, $n=96$) and 27% of the embryos co-treated with A23187 and KN62 (6% straight and 21% reversed, $n=108$) underwent abnormal cardiac looping ($P<0.05$) (Fig. 7B). Similarly, only 26% (11% straight and 15% reversed, $n=85$) and 24% (6% straight and 18% reversed, $n=98$) of the α2 and Ncx4a morphants treated with KN62 developed cardiac looping defects, respectively ($P<0.01$) (Fig. 7B). We further analyzed whether the suppression of the LR defects was due to the restoration of cilia motility and directional fluid flow in KV. Of the 13 embryos analyzed by high-speed videomicroscopy, we

observed active KV ciliary rotation in nine KN62-treated α2 morphants (see Movie 5 in the supplementary material). Moreover, 17 out of the 24 KN62-treated α2 morphants that were successfully implanted with fluorescent beads displayed counterclockwise fluid flow (Table 2; see Movie 6 in the supplementary material). These data clearly demonstrate that blocking the activity of CaMKII, a downstream signaling molecule for calcium, suppresses LR defects induced by thapsigargin, A23187, α2-MO or Ncx4a-MO. These data support the notion that Na,K-ATPase α2 and Ncx4a regulate zebrafish LR patterning by controlling levels of intracellular Ca^{2+} and indicate that CaMKII mediates calcium signaling at an early step of LR patterning.

DISCUSSION

Earlier biochemical and physiological studies have illustrated crucial roles of Na,K-ATPase and NCX in modulating intracellular Ca^{2+} levels (for reviews, see Blanco and Mercer, 1998; Blaustein and Lederer, 1999), but their roles during development have remained largely unknown. We now show that Na,K-ATPase α2 and Ncx4a function upstream of Nodal signaling to control zebrafish LR patterning. Knocking down the activities of these genes disrupts the normal expression patterns of laterality genes in the LPM and randomizes the placement of the internal organs. Since no apparent morphological defects other than the randomization of organ laterality were noted in α2 and Ncx4a morphants, the LR defects observed in these embryos are likely to be direct effects of downregulation of expression of Na,K-ATPase α2 and Ncx4a rather than secondary consequences of gastrulation and/or midline abnormalities.

We observed an unusual discordant expression pattern of *spaw* and *lft1/2* in α2 and Ncx4a morphants and A23187-treated embryos. In general, the expression of *lft1/2* follows that of *nodal* both temporally and spatially (for a review, see Schier, 2003). Of the zebrafish mutants and morphants examined thus far, randomized *spaw* is associated with randomized *lft1/2* expression, and loss of *spaw* expression is associated with the absence of *lft1/2* expression (Bisgrove et al., 2000; Bisgrove et al., 2005; Essner et al., 2005; Kramer-Zucker et al., 2005). However, this concordant expression pattern is disrupted in α2 and Ncx4a morphants, where *spaw* and *pitx2* are randomized but the expression of *lft1/2* in LPM is usually missing. It is likely that the absence of *lft1/2* expression in the lateral plate mesoderm and habenula of α2 and Ncx4a morphants or A23187-treated embryos is a consequence of the laterality defects because *lft1/2* expression in other tissues of these embryos is unaffected. How the concordant expression pattern of laterality genes was lost in these embryos is currently unknown, but this unusual phenotype indicates that multiple regulatory mechanisms are involved in the asymmetric expression of *lft1/2* in the LPM.

We present four lines of evidence supporting the notion that Na,K-ATPase α2 and Ncx4a modulate calcium signaling in DFCs/KV and thereby regulate LR patterning in zebrafish. First, although the sensitivity of our current imaging technology prevented us from measuring intracellular Ca^{2+} levels specifically in DFCs, we were able to measure Ca^{2+} levels in blastomeres. We observed a significant elevation of intracellular Ca^{2+} levels in blastomeres of α2 and Ncx4a morphants. This result is consistent with the roles of NCX and Na,K-ATPase in regulating intracellular Ca^{2+} levels delineated by numerous biochemical and physiological studies in cultured cells and in mammals (Blanco and Mercer, 1998; Blaustein and Lederer, 1999), and indicates that like their mammalian counterparts, Na,K-ATPase α2 and Ncx4a are involved in maintaining calcium homeostasis in zebrafish. Second, we manipulated intracellular Ca^{2+} levels with two chemicals used widely for this purpose. A23187 is a calcium ionophore that increases intracellular Ca^{2+} levels in intact cells by allowing extracellular calcium to cross the cell membrane. Thapsigargin is a SERCA-inhibitor that prevents Ca^{2+} from being resequestered into the ER/SR. Both of these treatments elevate intracellular Ca^{2+} levels. We found that embryos treated with a low dose of A23187 or thapsigargin are phenotypically identical to α2 and Ncx4a morphants. These embryos have no apparent morphological defects other than randomization of the placement of the internal organs. These embryos also share the unusual discordant *spaw* and *lft1/2* expression phenotype with α2 and Ncx4a morphants, implying that the LR defects of α2 and Ncx4a morphants are the result of imbalanced intracellular calcium. Third, we showed that constitutive activation of CaMKII causes LR defects in zebrafish, and that inhibiting CaMKII activity with KN62 is able to suppress LR defects (as induced by α2-MO, Ncx4a-MO, A23187 and thapsigargin) at a concentration that does not cause any additional morphological defects in the developing zebrafish embryos. These observations indicate that the LR defects induced by Ca^{2+} perturbation are at least in part mediated by CaMKII. Finally, targeting α2- and Ncx4a-MOs to DFCs is sufficient to disrupt asymmetric expression of *spaw*, *lft1/2* and *pitx2* and to randomize the placement of the internal organs, demonstrating an essential role of calcium homeostasis in DFCs/KV in zebrafish LR patterning. An emerging theme from recent studies suggests that the directional nodal flow and asymmetric calcium signaling around the node are fundamental to LR decisions in both mouse and zebrafish (McGrath et al., 2003; Bisgrove et al., 2005; Essner et al., 2005; Kramer-Zucker et al., 2005; Sarmah et al., 2005). Our findings that elevated Ca^{2+} levels in DFCs can immobilize KV cilia, abolish KV fluid flow and randomize the placement of the internal organs indicate that in addition to asymmetric signaling around the node, calcium influences zebrafish LR patterning by regulating the function of KV cilia.

The movement of eukaryotic flagella and cilia is in part regulated by intraflagellar calcium. For example, increased intracellular Ca^{2+} levels change the *Chlamydomonas* flagellar waveform (Hyams and Borisy, 1978; Bessen et al., 1980), whereas the elevation of intracellular Ca^{2+} levels can ultimately make sea urchin sperm flagella immobile (Brokaw, 1979; Gibbons and Gibbons, 1980). Our study showed that intracellular Ca^{2+} levels also regulate ciliary motility in KV in zebrafish, suggesting a conserved role of calcium in cilia motility. Although the precise mechanisms by which calcium signaling regulates ciliary function in KV requires further investigation, our study provides evidence that signaling mediated by CaMKII has an important role. It is possible that the activation of CaMKII represses the expression of certain genes required for ciliary function. Alternatively, calcium might modulate ciliary motility at a post-translational level, a notion supported by the finding that the binding of dynein to microtubules is modulated by calcium, which in turn affects the movement of *Chlamydomonas* flagella and sea urchin sperm axonemes (Nakano et al., 2003; Wargo et al., 2004; Wargo et al., 2005). It will be important to investigate whether a similar mechanism applies to KV ciliary motility. Furthermore, it has been shown that forced expression of inversin leads to LR defects and this effect is dependent on a physical interaction of INVS and calmodulin via the IQ domain, which is negatively regulated by the presence of calcium (Yasuhiko et al., 2001; Morgan et al., 2002), raising the possibility that calcium signaling directly modulates protein activities. Further investigation

of the mechanisms by which calcium signaling modulates ciliary motility will deepen our understanding of LR patterning, and should help to clarify whether this aspect of LR patterning is conserved among vertebrates.

We show that Na,K-ATPase α2 and Ncx4a influence LR decisions in zebrafish by modulating intracellular Ca^{2+} levels in DFCs/KV. The finding that Ncx1 is asymmetrically expressed on the right-hand side of Hensen's node during gastrulation in the chick suggests that these calcium-handling proteins might be involved in LR decisions in other vertebrate species (Linask et al., 2001). Currently, NCX1, NCX2, Na,K-ATPase α1 and α2 knockout mice are available, but no LR defects in these lines have been documented (James et al., 1999; Cho et al., 2000; Wakimoto et al., 2000; Koushik et al., 2001; Reuter et al., 2002). It will be important to re-evaluate the expression pattern of laterality genes in these mice to assess their roles in LR patterning in mammals. Alternatively, using Na,K-ATPase and NCX to modulate LR-related Ca^{2+} signaling might be a fish-specific mechanism. Owing to the partial genome duplication in teleosts, more Na,K-ATPase and NCX genes exist in the zebrafish than in the mammalian genome (nine Na,K-ATPase α-subunits and six NCX genes in zebrafish versus four Na,K-ATPase α-subunits and three NCX genes in mammals) (Blanco and Mercer, 1998; Blaustein and Lederer, 1999; Rajarao et al., 2001; Serluca et al., 2001; Blasiole et al., 2002; Canfield et al., 2002), and Ncx4a belongs to a subgroup of NCX genes that only exists in fish (our study) (Marshall et al., 2005). Therefore, it is conceivable that calcium homeostasis in the node might be regulated by other calcium-handling proteins in mammals. Analyzing whether Na,K-ATPase and NCX are important for regulating the intracellular Ca^{2+} level in ciliated nodal cells and whether a CaMKII-dependent pathway modulates nodal ciliary motility in other vertebrates will provide insight into the conservation of these pathways.

We thank K. Philipson, K. Hill and C. Nguyen for discussion and critical comments on the manuscript; Y. Wang and E. Stefani for access to the confocal microscope; J. M. Chen, C. M. Ho and A. Sagasti for access to the high-speed video camera. X.S. was supported by a postdoctoral fellowship from the American Heart Association Western States Affiliate (0425205Y). This work was supported by grants from the NIH (HD041367), American Heart Association Western States Affiliate (0555019Y) and the Laubisch Fund to J.-N.C. The Ncx4a sequences reported in this paper have been deposited in the GenBank database (accession number: EF470289).

Supplementary material

Supplementary material for this article is available at http://dev.biologists.org/cgi/content/full/134/10/1921/DC1

References

Adams, D. S., Robinson, K. R., Fukumoto, T., Yuan, S., Albertson, R. C., Yelick, P., Kuo, L., McSweeney, M. and Levin, M. (2006). Early, H^+-V-ATPase-dependent proton flux is necessary for consistent left-right patterning of non-mammalian vertebrates. *Development* **133**, 1657-1671.

Amack, J. D. and Yost, H. J. (2004). The T box transcription factor no tail in ciliated cells controls zebrafish left-right asymmetry. *Curr. Biol.* **14**, 685-690.

Berridge, M. J., Lipp, P. and Bootman, M. D. (2000). The versatility and universality of calcium signalling. *Nat. Rev. Mol. Cell Biol.* **1**, 11-21.

Bessen, M., Fay, R. B. and Witman, G. B. (1980). Calcium control of waveform in isolated flagellar axonemes of Chlamydomonas. *J. Cell Biol.* **86**, 446-455.

Bisgrove, B. W. and Yost, H. J. (2001). Classification of left-right patterning defects in zebrafish, mice, and humans. *Am. J. Med. Genet.* **101**, 315-323.

Bisgrove, B. W., Essner, J. J. and Yost, H. J. (2000). Multiple pathways in the midline regulate concordant brain, heart and gut left-right asymmetry. *Development* **127**, 3567-3579.

Bisgrove, B. W., Snarr, B. S., Emrazian, A. and Yost, H. J. (2005). Polaris and Polycystin-2 in dorsal forerunner cells and Kupffer's vesicle are required for specification of the zebrafish left-right axis. *Dev. Biol.* **287**, 274-288.

Blanco, G. and Mercer, R. (1998). Isozymes of the Na-K-ATPase: heterogeneity in structure, diversity in function. *Am. J. Physiol.* **275**, F633-F650.

Blasiole, B., Canfield, V., Degrave, A., Thisse, C., Thisse, B., Rajarao, J. and Levenson, R. (2002). Cloning, mapping, and developmental expression of a sixth zebrafish Na,K-ATPase alpha1 subunit gene (atp1a1a.5). *Gene Expr. Patterns* **2**, 243-246.

Blaustein, M. and Lederer, W. (1999). Sodium/calcium exchange: its physiological implications. *Physiol. Rev.* **79**, 736-854.

Brickey, D. A., Bann, J. G., Fong, Y. L., Perrino, L., Brennan, R. G. and Soderling, T. R. (1994). Mutational analysis of the autoinhibitory domain of calmodulin kinase II. *J. Biol. Chem.* **269**, 29047-29054.

Brokaw, C. J. (1979). Calcium-induced asymmetrical beating of triton-demembranated sea urchin sperm flagella. *J. Cell Biol.* **82**, 401-411.

Bunney, T. D., De Boer, A. H. and Levin, M. (2003). Fusicoccin signaling reveals 14-3-3 protein function as a novel step in left-right patterning during amphibian embryogenesis. *Development* **130**, 4847-4858.

Burdine, R. D. and Schier, A. F. (2000). Conserved and divergent mechanisms in left-right axis formation. *Genes Dev.* **14**, 763-776.

Canfield, V., Loppin, B., Thisse, B., Thisse, C., Postlethwait, J., Mohideen, M., Rajarao, S. and Levenson, R. (2002). Na,K-ATPase alpha and beta subunit genes exhibit unique expression patterns during zebrafish embryogenesis. *Mech. Dev.* **116**, 51-59.

Capdevila, J., Vogan, K. J., Tabin, C. J. and Izpisua Belmonte, J. C. (2000). Mechanisms of left-right determination in vertebrates. *Cell* **101**, 9-21.

Chen, J. and Fishman, M. (1996). Zebrafish tinman homolog demarcates the heart field and initiates myocardial differentiation. *Development* **122**, 3809-3816.

Chen, J., van Eeden, F., Warren, K., Chin, A., Nusslein-Volhard, C., Haffter, P. and Fishman, M. (1997). Left-right pattern of cardiac BMP4 may drive asymmetry of the heart in zebrafish. *Development* **124**, 4373-4382.

Cho, C.-H., Kim, S., Jeong, M., Lee, C. and Shin, H. (2000). The Na^+-Ca^{2+} exchanger is essential for embryonic heart development in mice. *Mol. Cells* **10**, 712-722.

Cooper, M. S. and D'Amico, L. A. (1996). A cluster of noninvoluting endocytic cells at the margin of the zebrafish blastoderm marks the site of embryonic shield formation. *Dev. Biol.* **180**, 184-198.

Ellertsdottir, E., Ganz, J., Durr, K., Loges, N., Biemar, F., Seifert, F., Ettl, A. K., Kramer-Zucker, A. K., Nitschke, R. and Driever, W. (2006). A mutation in the zebrafish Na,K-ATPase subunit atp1a1a.1 provides genetic evidence that the sodium potassium pump contributes to left-right asymmetry downstream or in parallel to nodal flow. *Dev. Dyn.* **235**, 1794-1808.

Essner, J. J., Vogan, K. J., Wagner, M. K., Tabin, C. J., Yost, H. J. and Brueckner, M. (2002). Conserved function for embryonic nodal cilia. *Nature* **418**, 37-38.

Essner, J. J., Amack, J. D., Nyholm, M. K., Harris, E. B. and Yost, H. J. (2005). Kupffer's vesicle is a ciliated organ of asymmetry in the zebrafish embryo that initiates left-right development of the brain, heart and gut. *Development* **132**, 1247-1260.

Fujinaga, M., Hoffman, B. B. and Baden, J. M. (1994). Receptor subtype and intracellular signal transduction pathway associated with situs inversus induced by alpha 1 adrenergic stimulation in rat embryos. *Dev. Biol.* **162**, 558-567.

Fukumoto, T., Kema, I. P. and Levin, M. (2005). Serotonin signaling is a very early step in patterning of the left-right axis in chick and frog embryos. *Curr. Biol.* **15**, 794-803.

Gibbons, B. H. and Gibbons, I. R. (1980). Calcium-induced quiescence in reactivated sea urchin sperm. *J. Cell Biol.* **84**, 13-27.

Hyams, J. S. and Borisy, G. G. (1978). Isolated flagellar apparatus of Chlamydomonas: characterization of forward swimming and alteration of waveform and reversal of motion by calcium ions in vitro. *J. Cell Sci.* **33**, 235-253.

James, P. F., Grupp, I. L., Grupp, G., Woo, A. L., Askew, G. R., Croyle, M. L., Walsh, R. A. and Lingrel, J. B. (1999). Identification of a specific role for the Na,K-ATPase alpha 2 isoform as a regulator of calcium in the heart. *Mol. Cell* **3**, 555-563.

Kawakami, Y., Raya, A., Raya, R. M., Rodriguez-Esteban, C. and Belmonte, J. C. (2005). Retinoic acid signalling links left-right asymmetric patterning and bilaterally symmetric somitogenesis in the zebrafish embryo. *Nature* **435**, 165-171.

Koushik, S., Wang, J., Rogers, R., Moskophidis, D., Lambert, N., Creazzo, T. and Conway, S. (2001). Targeted inactivation of the sodium-calcium exchanger (Ncx1) results in the lack of a heartbeat and abnormal myofibrillar organization. *FASEB J.* **15**, 1209-1211.

Kramer-Zucker, A. G., Olale, F., Haycraft, C. J., Yoder, B. K., Schier, A. F. and Drummond, I. A. (2005). Cilia-driven fluid flow in the zebrafish pronephros, brain and Kupffer's vesicle is required for normal organogenesis. *Development* **132**, 1907-1921.

Langenbacher, A., Dong, Y., Shu, X., Choi, J., Nicoll, D., Goldhaber, J., Philipson, K. and Chen, J. (2005). Mutation in sodium-calcium exchanger 1 (NCX1) causes cardiac fibrillation in zebrafish. *Proc. Natl. Acad. Sci. USA* **102**, 17699-17704.

Levin, M., Thorlin, T., Robinson, K. R., Nogi, T. and Mercola, M. (2002). Asymmetries in H^+/K^+-ATPase and cell membrane potentials comprise a very early step in left-right patterning. *Cell* **111**, 77-89.

Linask, K., Han, M., Artman, M. and Ludwig, C. (2001). Sodium-calcium exchanger (NCX-1) and calcium modulation: NCX protein expression patterns and regulation of early heart development. *Dev. Dyn.* **221**, 249-264.
Long, S., Ahmad, N. and Rebagliati, M. (2003). The zebrafish nodal-related gene southpaw is required for visceral and diencephalic left-right asymmetry. *Development* **130**, 2303-2316.
Marshall, C. R., Fox, J. A., Butland, S. L., Ouellette, B. F., Brinkman, F. S. and Tibbits, G. F. (2005). Phylogeny of Na^+/Ca^{2+} exchanger (NCX) genes from genomic data identifies new gene duplications and a new family member in fish species. *Physiol. Genomics* **21**, 161-173.
Marszalek, J. R., Ruiz-Lozano, P., Roberts, E., Chien, K. R. and Goldstein, L. S. (1999). Situs inversus and embryonic ciliary morphogenesis defects in mouse mutants lacking the KIF3A subunit of kinesin-II. *Proc. Natl. Acad. Sci. USA* **96**, 5043-5048.
McGrath, J. and Brueckner, M. (2003). Cilia are at the heart of vertebrate left-right asymmetry. *Curr. Opin. Genet. Dev.* **13**, 385-392.
McGrath, J., Somlo, S., Makova, S., Tian, X. and Brueckner, M. (2003). Two populations of node monocilia initiate left-right asymmetry in the mouse. *Cell* **114**, 61-73.
Morgan, D., Goodship, J., Essner, J. J., Vogan, K. J., Turnpenny, L., Yost, H. J., Tabin, C. J. and Strachan, T. (2002). The left-right determinant inversin has highly conserved ankyrin repeat and IQ domains and interacts with calmodulin. *Hum. Genet.* **110**, 377-384.
Nakano, I., Kobayashi, T., Yoshimura, M. and Shingyoji, C. (2003). Central-pair-linked regulation of microtubule sliding by calcium in flagellar axonemes. *J. Cell Sci.* **116**, 1627-1636.
Nonaka, S., Tanaka, Y., Okada, Y., Takeda, S., Harada, A., Kanai, Y., Kido, M. and Hirokawa, N. (1998). Randomization of left-right asymmetry due to loss of nodal cilia generating leftward flow of extraembryonic fluid in mice lacking KIF3B motor protein. *Cell* **95**, 829-837.
Okada, Y., Nonaka, S., Tanaka, Y., Saijoh, Y., Hamada, H. and Hirokawa, N. (1999). Abnormal nodal flow precedes situs inversus in iv and inv mice. *Mol. Cell* **4**, 459-468.
Okada, Y., Takeda, S., Tanaka, Y., Belmonte, J. C. and Hirokawa, N. (2005). Mechanism of nodal flow: a conserved symmetry breaking event in left-right axis determination. *Cell* **121**, 633-644.
Pfleiderer, P. J., Lu, K. K., Crow, M. T., Keller, R. S. and Singer, H. A. (2004). Modulation of vascular smooth muscle cell migration by calcium/ calmodulin-dependent protein kinase II-delta 2. *Am. J. Physiol. Cell Physiol.* **286**, C1238-C1245.
Rajarao, S., Canfield, V., Mohideen, M., Yan, Y., Postlethwait, J., Cheng, K. and Levenson, R. (2001). The repertoire of Na,K-ATPase alpha and beta subunit genes expressed in the zebrafish, Danio rerio. *Genome Res.* **11**, 1211-1220.
Raya, A. and Belmonte, J. C. (2006). Left-right asymmetry in the vertebrate embryo: from early information to higher-level integration. *Nat. Rev. Genet.* **7**, 283-293.
Raya, A., Kawakami, Y., Rodriguez-Esteban, C., Ibanes, M., Rassidin-Gutman, D., Rodriguez-Leon, J., Buscher, D., Feijo, J. and Izpisua Belmonte, J. (2004). Notch activity acts as a sensor for extracellular calcium during vertebrate left-right determination. *Nature* **427**, 121-128.
Reuter, H., Henderson, S., Han, T., Ross, R., Goldhaber, J. and Philipson, K. (2002). The Na^+-Ca^{2+} Exchanger is essential for the action of cardiac glycosides. *Circ. Res.* **90**, 305-308.
Ro, H., Soun, K., Kim, E. J. and Rhee, M. (2004). Novel vector systems optimized for injecting in vitro-synthesized mRNA into zebrafish embryos. *Mol. Cells* **17**, 373-376.
Sarmah, B., Latimer, A. J., Appel, B. and Wente, S. R. (2005). Inositol polyphosphates regulate zebrafish left-right asymmetry. *Dev. Cell* **9**, 133-145.
Schier, A. F. (2003). Nodal signaling in vertebrate development. *Annu. Rev. Cell Dev. Biol.* **19**, 589-621.
Serluca, F., Sidow, A., Mably, J. and Fishman, M. (2001). Partitioning of tissue expression accompanies multiple duplications of the Na^+/K^+ ATPase alpha subunit gene. *Genome Res.* **11**, 1625-1631.
Shiratori, H. and Hamada, H. (2006). The left-right axis in the mouse: from origin to morphology. *Development* **133**, 2095-2104.
Shu, X., Cheng, K., Patel, N., Chen, F., Joseph, E., Tsai, H. and Chen, J. (2003). Na,K-ATPase is essential for embryonic heart development in the zebrafish. *Development* **130**, 6165-6173.
Tabin, C. J. and Vogan, K. J. (2003). A two-cilia model for vertebrate left-right axis specification. *Genes Dev.* **17**, 1-6.
Takeda, S., Yonekawa, Y., Tanaka, Y., Okada, Y., Nonaka, S. and Hirokawa, N. (1999). Left-right asymmetry and kinesin superfamily protein KIF3A: new insights in determination of laterality and mesoderm induction by $kif3A^{-/-}$ mice analysis. *J. Cell Biol.* **145**, 825-836.
Tanaka, Y., Okada, Y. and Hirokawa, N. (2005). FGF-induced vesicular release of Sonic hedgehog and retinoic acid in leftward nodal flow is critical for left-right determination. *Nature* **435**, 172-177.
Toyoizumi, R., Kobayashi, T., Kikukawa, A., Oba, J. and Takeuchi, S. (1997). Adrenergic neurotransmitters and calcium ionophore-induced situs inversus viscerum in Xenopus laevis embryos. *Dev. Growth Differ.* **39**, 505-514.
Wakimoto, K., Kobayashi, K., Kuro-o, M., Yao, A., Iwamoto, T., Yanaka, N., Kita, S., Nishida, A., Azuma, S., Toyoda, Y. et al. (2000). Targeted disruption of Na^+/Ca^{2+} exchanger gene leads to cardiomyocyte apoptosis and defects in heartbeat. *J. Biol. Chem.* **275**, 36991-36998.
Wargo, M. J., McPeek, M. A. and Smith, E. F. (2004). Analysis of microtubule sliding patterns in Chlamydomonas flagellar axonemes reveals dynein activity on specific doublet microtubules. *J. Cell Sci.* **117**, 2533-2544.
Wargo, M. J., Dymek, E. E. and Smith, E. F. (2005). Calmodulin and PF6 are components of a complex that localizes to the C1 microtubule of the flagellar central apparatus. *J. Cell Sci.* **118**, 4655-4665.
Westerfield, M. (1995). *The Zebrafish Book. A Guide for the Laboratory Use of Zebrafish (Danio rerio).* Eugene: University of Oregon.
Yasuhiko, Y., Imai, F., Ookubo, K., Takakuwa, Y., Shiokawa, K. and Yokoyama, T. (2001). Calmodulin binds to inv protein: implication for the regulation of inv function. *Dev. Growth Differ.* **43**, 671-681.